Journal of Hydroscience and Hydraulic Engineering
Vol. 3, No. 2, November, 1985, pp.1-13.

RESUSPENSIION RATE FUNCTION FOR COHESIVE SEDIMENTS IN STREAM

By

Kuninori Otsubo and Kohji Muraoka

Division of Water and Soil Environment
National Institute for Environmental Studies, Tsukuba Science City, Japan

SYNOPSIS

In shallow lakes or estuaries, cohesive bottom sediments undergo repeated deposition and resuspension. They are suspended by current and wave motion, and dissolved nutrients in the bottom sediment pores are released into the upper waterbody. To estimate the released nutrient, it is essential to determine the amount of resuspended sediment. In this paper, the resuspension rate is studied experimentally and theoretically. We applied dimensional analysis to experimental results to obtain the dimensionless function of the resuspension rate against bed shear stress. Furthermore, we made a physical model to estimate the resuspension rate. Cohesive sediments are thought to be dislodged from the bottom by different three styles of detachment; sliding, lifting and rolling. We determined that for cohesive sediments sliding detachment predominates. By establishing the equation of motion for sliding sediment, and considering the fluctuations of the tractive force, we deduced the dimensionless resuspension rate function and compared the theoretical predictions with experimental results.

INTRODUCTION

There are two different viewpoints on the resuspension of cohesive sediment; continuous body or aggregation of cohesive particles (which have various forms and sizes). We have adopted the latter on the basis of our past study (7). The elementary factors to consider for this viewpoint are the critical shear stress, the resuspension rate and the duration of the suspension period of the cohesive sediments. In this paper, we discuss the resuspension rate. Cohesive sediments, having very small particle size and containing 10 - 20 % organic matter, show strong cohesive and weak gravitational resistance against current. It is very difficult to estimate the cohesive resistance quantitatively at the inter-particle power level. In order to estimate it, we used the viscosity and yield stress, which are macroscopic parameters showing the physical properties of cohesive sediments as a continuous body, assuming that they reflect the inter-particle cohesive bond. We propose a model for the apparent density ρ_0 and diameter d_0 for representative flocculated sediments concerning detachment phenomenon.

The resuspension rate p_m is defined as follows:

$$p_m = (p_0\hat{t}_0/t_d)(1/\hat{t}_0) = p_0/t_d \qquad (1)$$

where p_0 = probability that $\tau > \tau_c$; $\hat{t}_0$ = time scale of fluctuation of bed shear stress , with which the incipient moion is considered; $p_0\hat{t}_0$ = duration time over which the bed shear stress can dislodge the sediments; t_d = duration time required for cohesive sediment to be dislodged. τ = bed shear stress by current; and τ_c = the so-called critical shear stress. We have to estimate p_0 and t_d in order to evaluate p_m theoretically. To estimate p_0, we took the fluctuation of τ into consideration, for t_d, we applied the equation of motion to the detachment of sediment from the bottom.

Since the predominant detachment style for cohesive sediments is sliding, we estimated t_d from the equation of motion for a cohesive sediment on the sliding

detachment condition and a statistical model of the fluctuation τ . Using p_0 and t_d , we deduced the theoretical function of dimensionless resuspension rate p_{m*}.

ANALYSIS OF EXPERIMENTAL RESUSPENSION RATE FOR COHESIVE SEDIMENTS

If the cohesive sediments are regarded as particles, p_{m*}, the dimensionless resuspension rate, is expressed as follows:

$$p_{m*} = (A_2/A_3)(P_m/\rho_0 d_0)t_0 = p_m t_0 \tag{2}$$

where A_2, A_3 = 2- and 3-dimensional geometrical coefficients of the sediment, respectively; ρ_0, d_0 = representative density and diameter of sediments at their incipient motion; P_m = resuspended mass per unit area per unit time; t_0 = characteristic time concerning resuspension phenomena. We considered two characteristic times: one is 'the time independent of the flow property'; the other, 'the time concerning mobility of particle to the flow'. The former is expressed as

$$t_{01} = \eta_1/[\rho(\rho_0/\rho-1)gd_0] \propto d_0/w_f \tag{3}$$

where η_1 = viscosity of sediments aggregation; ρ = density of water; g = gravitational acceleration; and w_f = falling velocity of sediment given by Stokes' law. The latter is expressed as

$$t_{02} = \eta_1/\tau(\propto d_0/v_0 \propto (d_0/u_d)(\eta_1/\mu)) \tag{4}$$

where v_0 = velocity of dislodged particle; u_d = local velocity at the representative height; and μ = viscosity of water. In Eq. 4, we assumed that $v_0 \propto u_d(\mu/\eta_1)$ for an hydraulically smooth surface condition and that $\tau \propto \mu(u_d/d_0)$. Substituting Eq. 3 and Eq. 4 into Eq. 2, we can define the following dimensionless parameters about resuspension rate.

$$p_{*1} = (\frac{A_2}{A_3})(\frac{P_m\eta_1}{\rho_0\rho(\rho_0/\rho-1)gd_0^2}) = p_m t_{01} \tag{5}$$

$$p_{*2} = (A_2/A_3)[(P_m\eta_1)/(\rho_0 d_0\tau)] = p_m t_{02} \tag{6}$$

Applying the experimental data for P_m into Eqs. 5 and 6, we can inspect the behaviors of p_{*1} and p_{*2} against the demensionless bed shear stress if the values of ρ_0 and d_0 are estimated.

Figure 1 (a) is a schematic figure of ρ_0 and d_0. We assumed here that the bottom is composed of flocculated sediments of diameter d_0 and density ρ_0, each of which consists of several individual particles of diameter d_m and density σ and bondage water. On the other hand, Fig. 1(b) shows the continuous body model for the bottom sediment. In this model, individual particles of diameter d_m and density σ are dispersed in the water and the bed is regarded as a one-phase colloidal solution of apparent density ρ_t.

Assuming that the flocculated sediments are packed in a simple cubic arrangement and that the pore spaces are filled with free water, we evaluated the value of ρ_0 as follows:

$$\rho_0 = (1/A_3)(\rho_t-\rho) + \rho \tag{7}$$

where

$$\rho_t = [\sigma(100+w)]/[100+(\sigma/\rho)w] \tag{8}$$

w = water content(%) of cohesive sediments aggregation. The value of A_3 is $\pi/6$ for a sphere and 1 for a cube. In the latter case, ρ_0 is equivalent to ρ_t. According to Eq. 7, ρ_0 is independent of the flocculated sediment diameter. This means that the number of individual particles of diameter d_m which make up the flocculated

sediment has no effect on ρ_0.

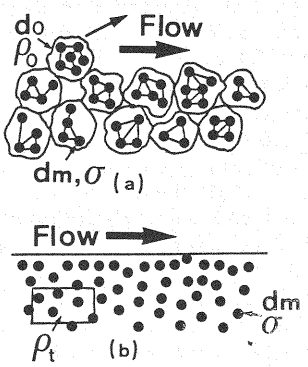

Fig. 1 Schmatic figures of ρ_0 and d_0

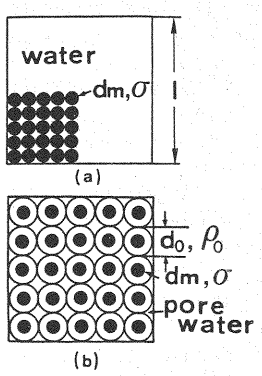

Fig. 2 Definition sketch of d_0

Figure 2 explains d_0. Let us consider a cube with volume ℓ^3. The substantial total volume of d_m size particles in this volume ℓ^3, V_s, is expressed as follows:

$$V_s = (100\rho\ell^3)/(100\rho+w\sigma) \tag{9}$$

The number of d_m size particles in volume ℓ^3, n_d, is written as

$$n_d = (1/A_3)(\ell/d_m)^3[(100\rho)/(100\rho+w\sigma)] \tag{10}$$

However n_d number of particles are not able to fill up volume ℓ^3 in a simple cubic arrangement, as shown in Fig. 2(a). We considered simply that a flocculated sediment is a complex of k numbers of d_m-size particles and bondage water. Then the number of flocculated sediments N_d is given as follows:

$$N_d = n_d/k = (1/k)(1/A_3)(\ell/d_m)^3[(100\rho)/(100\rho+w\sigma)] \tag{11}$$

We assumed that N_d pieces of flocculated sediment fill up volume ℓ^3 in a simple cubic arrangement and defined the diameter of each N_d piece as the representative diameter d_0. Hence, d_0 is written as

$$d_0 = (1/N_d)^{1/3}\ell = (kA_3)^{1/3}[(100\rho+w\sigma)/(100\rho)]^{1/3}d_m \tag{12}$$

Table.1 Values of representative density, ρ_0, and diameter, d_0

	Lk. Kasumi sediment G_s = 2.28, d_m = 27.7 μm					Kaolinite clay G_s = 2.6, d_m = 6.5 μm				
w(%)	1450	1200	1080	980	790	360	300	250	200	150
ρ_t(t/m^3)	1.03	1.04	1.045	1.050	1.053	1.15	1.18	1.21	1.25	1.32
ρ_0(t/m^3)	1.06	1.08	1.09	1.10	1.12	1.29	1.34	1.40	1.49	1.61
d_0(μm)	72.6	68.7	66.0	64.0	60.0	11.4	10.9	10.3	9.6	8.9
d_0/d_m	2.62	2.48	2.38	2.31	2.15	1.76	1.67	1.58	1.48	1.37

G_s = specific gravity of bottom sediment or clay; d_m = mean diameter;
w = water content in percent of dry weight.

According to Eq. 12, d_0 increases with increasing of water content and the number of original d_m-size particles in the flocculated sediment. Since it is difficult to determine how many particles are contained in a flocculated sediment, we assumed that it consists of one particle and bondage water as shown in Fig. 2(b). Table 1 shows the values of ρ_t, ρ_0, d_0 (for k = 1) and d_0/d_m of precipitation matter in Lake Kasumi and Kaolinite, for given water contents. The water contents listed in Table 1, varying with the sediment type as shown, are the possible values near bottom surface for a usual accumulation process. We measured the diameters of sediments suspended in flow and found that they were 1.2 - 2.0 times larger than the original diameters (7). From the above we can conclude that d_0 values shown in Table 1 are useful to study sediment detachment. However, other models are possible and the mechanism of flocculation should be carefully studied in future.

Figure 3 shows examples of the relations between p_{*1} and (τ/τ_{c2}). The experimental data are scattered depending upon water content even for the same kind of sediment, and more widely scattered for different kinds of sediment. For experimental data on P_m versus τ, please refer to Reference (7). On the other hand, the relations between p_{*2} and τ/τ_{c2} vary little with water content condition for the same sediment. In Fig. 4, approximate linear relations are drawn between p_{*2} and τ/τ_{c2} on a log-log scale for eight different sediments. Though the lines are somewhat scattered, they can be grouped as a formulation independent of sediment kind as follows:

$$p_{*2} = C_2(\tau/\tau_{c2})^{\alpha_2} \qquad (13)$$

where C_2, α_2 = experimental coefficients. Using the characteristic time t_{02}, we are able to obtain the resuspension rate function experimentally, independently of water content and sediment kind (8).

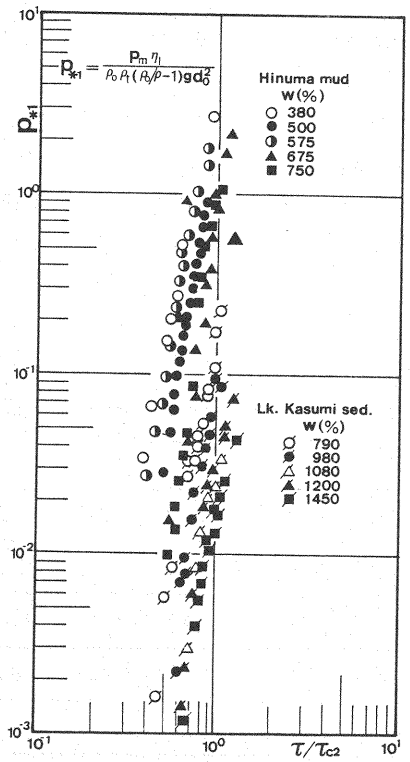

Fig. 3 Relations between p_{*1} and τ/τ_{c2}

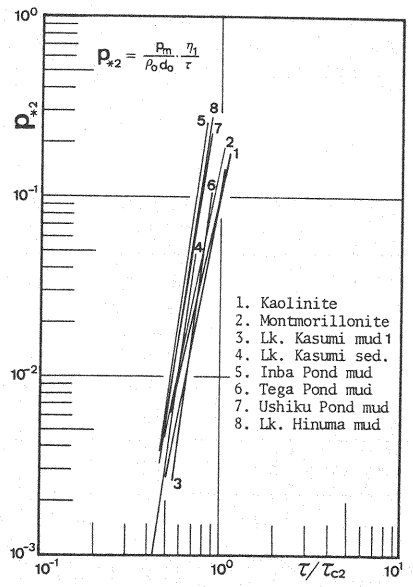

Fig. 4 Approximate relations between p_{*2} and τ/τ_{c2}

DETACHMENT STYLE FOR COHESIVE SEDIMENTS

The results of Fig. 4 show that the viscosity is a very important factor controlling the resuspension rate. Viscosity is a representative property of material in flowing conditions; therefore, it is not correct to analyze the resuspension process as an instantaneous phenomena in which the static balance between the tractive force and resistance forces breaks down. Since detachment of the sediment from a bed takes some time, we should deduce the resuspension rate p_m on the basis of the the equation of motion for a dislodged sediment. To express the detachment motion of cohesive sediment kinematically, we have to decide first what the predominant detachment style is. A particle is torn up from the bed into the water by the lift force under the condition of rolling and lifting detachment, and is torn away from the bed by shear force under the condition of sliding detachment. According to our preceding study, the gravitational resistance against the current is negligible in the case of cohesive sediment (9). Evaluating the impulses (defined as the product of force and time), which act on a sediment to tear up and away, and comparing the two impulses, we determined the predominant detachment style.

Figure 5 (a) and (b) is a sketch of the tear-up and tear-away processes, respectively, in the contact section between the detaching particle and the bottom. A cylindrical coordinate system is introduced: the origin is the center of the contact section; and the axes of r and θ are taken in the horizontal plane. For simplicity, the contact section is assumed to be a disk, whose area is $(\pi/4)d_*^2$ and thickness is h_*, at the initial stage of detachment. It is also assumed that the contact section is filled with cohesive material of viscosity η_1.

In Fig. 5(a), we assume that tear-up detachment is completed when the distance h_f of the contact section approaches infinity. The behavior of the cohesive matter in the horizontal plane is assumed to be isotropic. The volume of cohesive matter, which passes through the lateral face section of the cylinder with radius r and thickness h_f per unit time, is expressed as

$$V_1 = 2\pi r(h_f^3/12\eta_1)(dP/dr) \tag{14}$$

where P = normal stress. The volume of transformation of contact section per unit time due to movement of the cohesive material is expressed by Eq. 15

$$V_2 = \pi r^2(dh_f/dt) \tag{15}$$

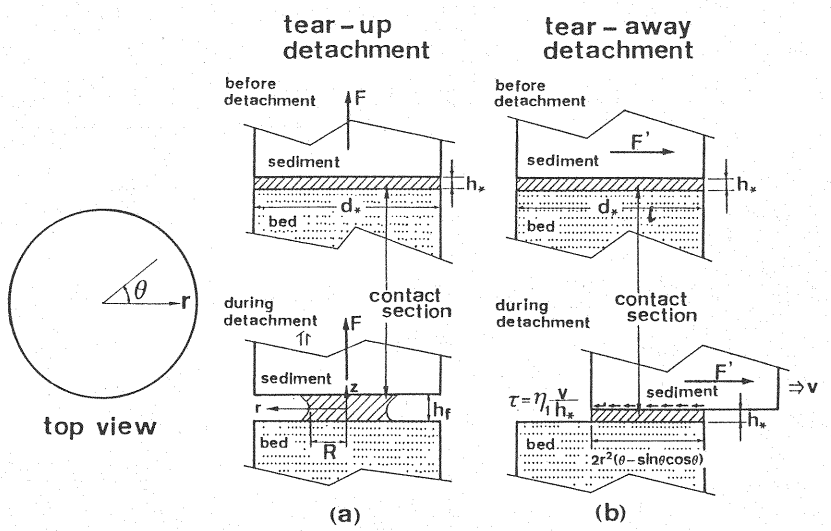

Fig. 5 Definition sketch of detachment styles

Because $V_1 = V_2$, the following equation is deduced.

$$dP/dr = (6\eta_1/h_f^3)(dh_f/dt)r \tag{16}$$

Integrating both sides of Eq. 16 with respect to r with the boundary condition P = 0 at r = R, we obtain the following expression for P.

$$P = (3\eta_1/h_f^3)(dh_f/dt)(r^2-R^2) \tag{17}$$

The tear-up force F has the the following relation with P.

$$F = \int_0^R 2\pi rP\, dr \tag{18}$$

Incorporating Eq. 17, Eq. 18 becomes

$$F = -(3\pi/2)R^4(\eta_1/h_f^3)(dh_f/dt) \tag{19}$$

The bulk V_* of cohesive material is constant during the tear-up process and it is expressed by

$$V_* = (\pi/4)d_*^2h_* = \pi R^2h_f \tag{20}$$

Substituting Eq. 20 into Eq. 19, and integrating both sides with respect to time on the condition that $h_f \to \infty$ at $t = t_d$, we obtain the impulse required for the sediment to be torn-up as follows:

$$Ft_d = -(3/8\pi)(V_*^2/h_*^4)\eta_1 = -(3\pi/128)(d_*^4/h_*^2)\eta_1 \tag{21}$$

Next, we discuss the impulse required for the sediment to be torn-away under the condition of sliding detachment. In Fig. 5(b), we assume that the shear stress is constant during the separation process, and consider that detachment is completed when the contact area between the detaching sediment and the bottom decreases to zero. The contact area A_c is defined as

$$A_c = 2r^2(\theta-\sin\theta\cos\theta)$$
$$= (d_*^2/2)[\arccos(t/t_d)-(t/t_d)(1-(t/t_d)^2)^{1/2}] \tag{22}$$

where t = time; and t_d = time when the detachment is completed. The impulse is expressed as follows:

$$\int_0^{t_d} F'\, dt = \int_0^{t_d} A_c\eta_1(dv/dz)\, dt \tag{23}$$

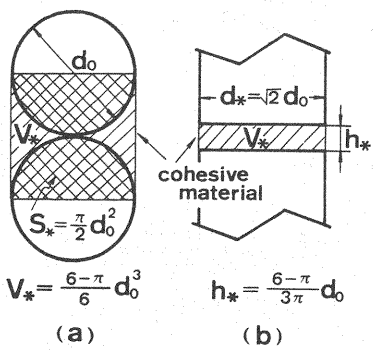

Fig.6 Dependence of F_* of $a_*(= h_*/d_*)$

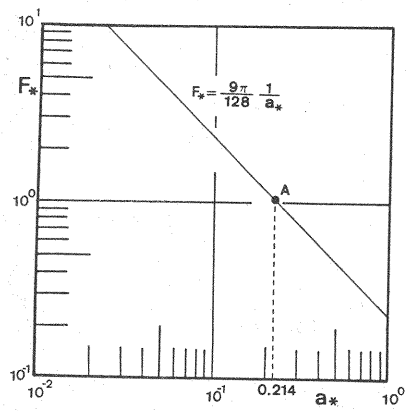

Fig. 7 Definition sketch

where F' = tear-away force; $\eta_1(dv/dz)$ = shear stress; and v = velocity of sliding sediment. Substituting the relation, $dv/dz = d_*/(h_* t_d)$, into Eq. 23, we obtain the impulse $\overline{F}t_d$ required for the sediment to be torn-away, as follows:

$$\overline{F}t_d = \int_0^{t_d} F' \, dt = (1/3)(d_*^3/h_*)\eta_1 \qquad (24)$$

where $\overline{F}$ = mean tractive force during the time of t_d.

Equations 21 and 24 show that the two impulses are independent of t_d. We judge which detachment style is more likely to occur by comparing the absolute values of both impulses; $|F|t_d$ and $|\overline{F}|t_d$.

$$(|F|t_d)/(|\overline{F}|t_d) = |F|/|\overline{F}| = F_*$$

$$= (9\pi d_*)/(128 h_*) \fallingdotseq 0.221(1/a_*) \qquad (25)$$

where $a_* = h_*/d_*$. Figure 6 shows the dependence of F_* on a_*. When $a_* < 9\pi/128$, $F_* > 1$. The smaller a_* is, the larger F_* becomes. Now, we imagine that sediments are packed in a simple cubic arrangement in which case a_* is a maximum. The pore volume V_* between two contacting sediments is expressed as $(6-\pi)d_0^3/6$; and the contact area of two facing sediments S_* is expressed as $(\pi/2)d_0^2$ (see Fig. 7). Because it is very difficult to estimate the distance h_* between two touching spheres (a), the model was simplified to two contacting disks (b). Representative thickness h_*, defined as V_*/S_*, is then given as $(6-\pi)d_0/3\pi$; and representative diameter d_*, defined as $\{(4/\pi)S_*\}^{1/2}$, as $\sqrt{2}d_0$. Substituting both values of h_* and d_* into Eq. 25, we obtain the following value of F_*.

$$F_* = (9\pi/128)[3\sqrt{2}\pi/(6-\pi)] \fallingdotseq 1.03 \qquad (a_* \fallingdotseq 0.221) \qquad (26)$$

This relation is plotted as point 'A' in Fig. 6. The above discussion shows that the impulse for tear-away is almost the same as for tear-up even for such a simple cubic arrangement. The condition, $a_* \ll 1$, is generally acceptable anytime the cohesive force predominates, which is exactly the case for cohesive sediments. Therefore, we conclude that sliding detachment (tear-away) is mostly likely, while rolling and lifting (tear-up) is unlikely for cohesive sediments. This conclusion is confirmed by observation of the detachment phenomenon, that is, the sediments were almost torn-away and then transported with sliding, rolling, sultating and suspending motion.

PREDICTION OF DIMENSIONLESS RESUSPENSION RATE FOR COHESIVE SEDIMENTS

As mentioned in the preceding section, the sediment's detachment does take place not instantaneously but gradually, thus we should use the equation of incipient motion to estimate the resuspension rate. In this sense, the basic method to deduce the resuspension rate for cohesive sediments is same as for sand particles (5). Differences between cohesive sediments and sands are as follows: for cohesive sediments, resistance force versus tractive force is not a gravitational force as it is for sand, but a cohesive force; a sediment reaches its equilibrium velocity as soon as it begins to move because the viscosity of sediment is so high that the inertia force is negligible, while for sands, the velocity increases gradually during detachment; according to the conclusion of the preceding section, the detachment style is most likely to be sliding for cohesive sediments, while for sands, all three detachment styles are possible.

Figure 8 shows the case where the tractive force D and resistance force R_v act on sediment A, and the sediment is about to be dislodged from the bed by sliding. For this case, the lifting and gravitational forces are neglected. The equation of streamwise motion for the sediment is written by follows:

$$A_3(1+C_M)(\rho_0-\rho)d_0^3(dv/dt) - k_3A_1\eta(u_d-u_c)d_0 + k_4A_1\mu v d_0 = 0 \qquad (27)$$

where A_1 = 1-dimensional geometrical coefficient of the sediment; C_M = added mass coefficient; k_3, k_4 = coefficients concerning tractive and resistance forces; u_c =

critical flow velocity; and η = viscosity of sediment aggregation. The second term of the left-hand side of Eq. 27, the tractive force, and the third one, the resistance force, are expressed by use of Stokes' law because d_0 is very small; the bottom bed is considered to be an hydraulically smooth surface; and η is very high.

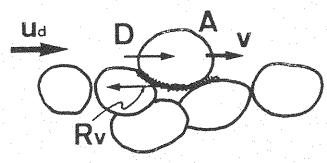

Fig. 8 Definition sketch

The solution of Eq. 27 is expressed by

$$v/v_0 = 1 - \exp(-k_4 A_0 \eta t) \tag{28}$$

where

$$A_0 = A_1/[A_3(1+C_M)(\rho_0-\rho)d_0^2] \tag{29}$$

and v_0 = equilibrium velocity of sediment given by

$$v_0 = (k_3/k_4)(\mu/\eta)(u_d-u_c) \tag{30}$$

Assuming that the tractive force acts on the upper half and the cohesive force acts on the lower half, $k_3 = k_4 = 1/2$. We can assume that a sediment moves with v_0 if T_d is much larger than t_p, where T_d = time required for the sediment to move the diameter length; t_p = time to accelerate the particle speed from zero to 90% of v_0. Using the value of ρ_0 and d_0 for the two models shown in Fig. 1, we calculated T_d/t_p values and listed them in Table 2. The values of t_p in Table 2 were calculated on the condition that it would become as high as possible; the values of T_d, as low as possible. As a result, we can approximate the sediment motion with an equilibrium velocity v_0.

Table.2 Values of t_p, T_d and T_d/t_p

	ρ_o (g/cm^3)	d (μm)	$A_0 \times 10^3$	$t_p \times 10^3$ (s)	$T_d \times 10^3$ (s)	T_d/t_p
(a)	1.2	38	4115	0.001	6.33	6330
(b)	2.3	20	2308	0.002	2.34	1670

For (a) and (b), see Fig. 1.

The resuspension rate of cohesive sediment (probability density per unit time for a cohesive sediment on the bed to be dislodged), p_m, is given as Eq. 1. We need to estimate p_0 and t_d in order to obtain the resuspension rate function. The probability p_0 for $\tau > \tau_c$, is expressed as

$$p_0 = [\int_{\tau_c}^{\infty} f(\tau)\, d\tau]/[\int_0^{\infty} f(\tau)\, d\tau] \tag{31}$$

where $f(\tau)$ = probability density function of bed shear stress. We define the sediment's detachment as follows: a sediment is not dislodged from the bottom bed until it slides a distance $a_1 d_0$ (where a_1 is coefficient). According to this definition, t_d is expressed as follows:

$$t_d = (a_1 d_0)/v_0 = (a_1 d_0 \eta)/(u_d-u_c)\mu \tag{32}$$

If an hydraulically smooth surface is assumed, the following equations are given in the viscous sublayer.

$$u_d = (a_2 d_0/\mu)\tau; \quad u_c = (a_2 d_0/\mu)\tau_c \tag{33}$$

where a_2 = coefficient; and $a_2 d_0$ = the representative height at which the tractive force acts. Substituting Eq. 33 into Eq. 32 and taking the statistical property of bed shear stress into consideration, we obtain

$$t_d = (a_1/a_2)[1/(E[\tau|\tau > \tau_c]-\tau_c)] \tag{34}$$

where $E[\tau|\tau>\tau_c]$ = conditional mean bed shear stress acting in time duration $p_0 t_0$. (Equation 34 can also be deduced for an hydraulically rough surface condition. In that case, we consider the tractive force to be proportional to $(u_d^2-u_c^2)$ and apply the logarithmic velocity-distribution law for a rough surface to the u/u_* function.) Assuming that the distribution of τ is Gaussian, we deduce the following for t_d.

$$t_d = \frac{a_1}{a_2}\frac{\eta}{\bar{\tau}}\left[1+\delta_0\frac{\Phi(y_c)}{p_0}-\frac{\tau_c}{\bar{\tau}}\right]^{-1} = \frac{a_1}{a_2}\frac{\eta}{\bar{\tau}}\, g\left(\frac{\bar{\tau}}{\tau_c}\right)^{-1} \tag{35}$$

where $\Phi(y)$ = the error function; $y_c = (\tau_c-\bar{\tau})/\sigma_0$; $\bar{\tau}$, σ_0 and δ_0 = mean value, standard deviation and variable coefficient of $f(\tau)$, respectively. Therefore, substituting Eq. 35 into Eq. 1, we deduce the dimensionless resuspension rate function for cohesive sediments as follows:

$$p_{m*} = (\eta/\bar{\tau})p_m = (a_2/a_1)g(\bar{\tau}/\tau_c)p_0 \tag{36}$$

Now, we rewrite $\bar{\tau}$ as τ in Eq. 36 for convenience. Figure 9 shows the dependence of p_{m*} on τ/τ_c calculated by use of Eqs. 31 and 36 with $a_1 = 1$, $a_2 = 0.75$ and $\delta_0 = 0.5$. The gradient of p_{m*} versus τ/τ_c is very high when $\tau/\tau_c < 1$, and low when $\tau/\tau_c > 1$; p_{m*} approaches a constant(= 0.75) when $\tau/\tau_c >> 1$. The assumptions about a Gaussian form for $f(\tau)$ and $\delta_0 = 0.5$ for an hydraulically smooth surface have not been confirmed. Probability density functions of shear stress, pressure and velocity fluctuations near the bottom bed for an hydraulically smooth surface have been investigated experimentally by Corcos (2), Willmarth & Wooldridge (10), Grass (4), and Blinco & Simons (1). No general conclusion can be drawn from these, but their results do not seem to conflict with our assumptions.

COMPARISON OF DIMENSIONLESS RESUSPENSION RATE FUNCTION WITH EXPERIMENTAL RESULTS

In a preceding studies (6), (7), we defined two critical shear stresses for cohesive sediments; the limit of sediment's movement, τ_{c1}, and that of bottom bed destruction, τ_{c2}. We have not mentioned which of these should be used for the critical shear stress, τ_c, in Eq. 36. In deducing Eq. 36, there is no necessity to choose between them. By taking the bed shear stress fluctuations into consideration, we can define the sediment resuspension even if the mean bed shear stress is less than the critical shear stress, τ_c. By inspecting which p_{m*} function i.e., that against τ/τ_{c1} or that against τ/τ_{c2}, coincides better with the experimental results, we tried to choose most suitable function. With the following relation between p_{m*} and P_m:

$$p_{m*} = (\eta/\tau)p_m = (\eta/\tau)(A_2/A_3)[P_m/(\rho_0 d_0)] \tag{37}$$

we rewrite the experimental data of P_m to dimensionless form, p_{m*}, by assuming that the sediment is a sphere ($A_2 = \pi/4$, $A_3 = \pi/6$) and by applying η_1 to η, Eq. 7 to ρ_0 and Eq. 12 to d_0. We inspect the dependence of p_{m*} on τ/τ_{c1} (Fig.10) and τ/τ_{c2} (Fig.11), respectively. In these figures, the symbols show the experimental data obtained under the water content conditions as shown in figures; the

dashed line is the theoretical resuspension rate curve given by Eq. 36. In Fig. 10, we should examine the region $\tau/\tau_{c1} > 1$ because when $\tau < \tau_{c1}$ the probability that the sediment will be dislodged is very small. In this case, the p_{m*} differs from τ/τ_{c1} with respect to not only the gradient but also the value itself. In Fig. 11, the region $\tau/\tau_{c2} < 1$ should be examined because the bed is

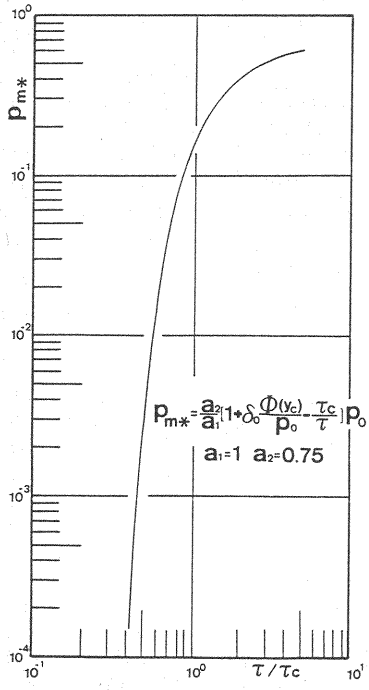

Fig. 9 Dimensionless resuspension rate function for cohesive sediments

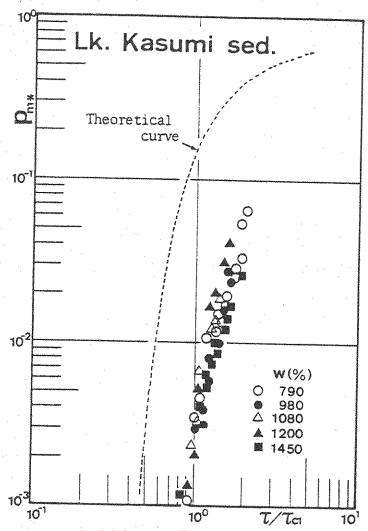

Fig. 10 Relations between p_{m*} and τ/τ_{c1}

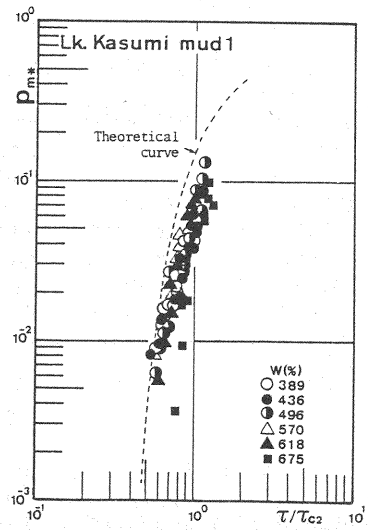

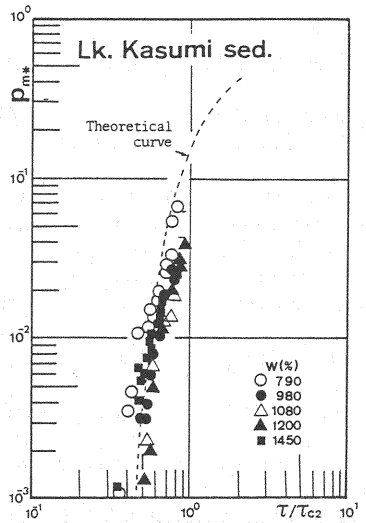

Fig. 11 Relations between p_{m*} and τ/τ_{c2}

violently destroyed by the current and Eq. 36 is not applicable when $\tau > \tau_{c2}$. In this region the theoretical and experimental result coincide well with each other. According to the above discussion, we conclude that τ_{c2} is more suitable for τ_c in Eq. 36. Using τ_{c2} as τ_c, we can estimate the resuspension rate of the cohesive sediment, p_{m*}, against τ/τ_c without the introduction of any physically meaningless coefficients. The results shown in Fig. 11 also give the reasonable support for choosing p_{*2} and τ/τ_{c2} in the experimental data shown in Fig. 4.

The characteristics of the resuspension rate function for cohesive sediments are as follows: it can be used when $\tau/\tau_{c2} < 1$, while for the pick-up rate of sand particles the function can be used when $\tau/\tau_c >= 1$. In cohesive sediments, when τ becomes larger than τ_{c2}, the sediments bed begins to flow not only at the surface layer but also at the inner layer, and is quickly and violently destroyed. In that bed condition, the tractive force would not act parallel to the bed surface, and moreover would be concentrated at some local section, thus the mechanism of resuspension at the time when $\tau/\tau_{c2} > 1$ would become so different from that at the time when $\tau/\tau_{c2} < 1$, that it would be impossible to apply Eq. 36 to the former case.

Equation 36 can be usd in the following conditions: the sediments forming the bottom bed has a yield value τ_{y1} (where τ_{y1} is related to τ_{c2} (6), (7)); its water content is high and its yield stress is less than 2 N/m^2. Many cohesive bottom sediments, especially those in lakes, satisfy the above conditions, therefore, Eq. 36 is generally applicable.

CONCLUSIONS

The results obtained in this paper are summarized below:

1) Cohesive bottom sediment can be considered to be an aggregation of cohesive particles of various forms and sizes. The diameter d_0 and density ρ_0 of the aggregation are expressed by Eqs. 7 and 12, respectively.

2) The experimental resuspension rate can be represented as shown in Fig.4, i.e., p_{*2} versus τ/τ_{c2}.

3) The predominant detachment style for cohesive sediments was determined to be sliding detachment.

4) A equation of motion was used to find a dimensionless resuspension rate function, p_{m*}. This function was found to show good agreement with experimental data when plotted against τ/τ_{c2}.

5) The dimensionless resuspension function (Eq. 36) is applicable when the cohesive sediments have a yield value and this yield value is less than 2 N/m^2. Since many cohesive sediments satisfy these conditions, e.g., most lake muds and estuary muds, the resuspension rate function found here has wide applicability.

ACKNOWLEDGEMENTS

We would like to thank Dr. P. G. Diosey for correcting the manuscript. We also would like to thank Mr. K. Hoshino for drawing the figures.

REFERENCES

1. Blinco, P.H. and D.B. Simons : Characteristics of turbulent boundary shear stress, Proc. ASCE, April, EM2, pp.203-220, 1974.
2. Corcos, G.M. : The structure of turbulent pressure field in boundary layer flows, J. Fluid Mech., Vol.18, pp.353-378, 1964.
3. Einstein, H.A. and E.A. El-Sami : Hydrodynamic forces on a rough wall. Review of Modern Physics, 21, pp.520-524, 1949.
4. Grass, G.M. : Structual feature of turbulent flow over smooth and rough boundaries, J. Fluid Mech., Vol.50, pp.233-260, 1971.
5. Nakagawa, H. and T. Tsujimoto : Study on mechanism of motion of individual sediment particles, Proc. JSCE, No.244, pp.71-80, 1975 (in Japanese).
6. Otsubo, K. and K. Muraoka : On the relation between physical properties and critical shear stress of mud, Proc. of the 25th Japanese Conference on Hydraulics, JSCE, pp.73-78, 1981 (in Japanese).

7. Otsubo, K. : Experimental studies on the physical properties of mud and the characteristics of mud transportation, Research Report from the National Institute for Environmental Studies, Japan, No.42, 1983 (in Japanese).
8. Otsubo, K. and K. Muraoka : Pick-up rate function for cohesive sediment in stream, Proc. of the 28th Japanese Conference on Hydraulics, JSCE, pp.671-677, 1984 (in Japanese).
9. Otsubo, K. : Study on mechanism of cohesive sediments resuspension, Doctral Thesis, Kyoto University, Dept. of Civil Engineering, 1985 (In Japanese).
10. Willmarth, W.W. and C.E. Wooldridge : Measurements of the fluctuating pressure at the wall beneath a thick turbulent boundary, J. Fluid Mech., Vol.14, pp.187-210, 1962.

APPENDIX - NOTATION

The following symbols are used in this paper:

a_1 = coefficient about the sliding distance of sediment in detachment;
a_2 = coefficient about the height of flow acting on particle;
a_* = h_*/d_* = ratio of height to diameter of modeled contact section;
A_0 = dimensional coefficient defined by Eq.(29);
A_1, A_2, A_3 = 1-, 2- and 3-dimensional geometrical coefficient of sediment;
A_c = contact area of two particles in detachment model;
C_2 = coefficient in Eq.(13);
C_M = added mass coefficient;
d_0 = representative diameter of sediments at their detachment;
d_m = mean diameter of sediment;
d_* = diameter of particles in detachment model;
D = tractive force in Fig. 8;
$f(\tau)$ = probability density function of bed shear stress;
F, F' = tear-up and tear-away forces;
$\overline{F}$ = time averaged value of F';
F_* = ratio of $|F|$ to $|\overline{F}|$;
g = gravitational acceleration;
$g(\overline{\tau}/\tau_c)$ = function defined by Eq.(35);
h_f = thickness of cohesive material at contact section in detachment;
h_* = initial thickness of cohesive material at contact section;
k = numbers of particles of diameter d_m in aggregated sediment;
k_3, k_4 = coefficient concerning tractive and resistant force;
ℓ = length of the member of fictitious cube;
n_d = numbers of d size particle in volume ℓ^3;
N_d = numbers of flocculated sediments in volume ℓ^3;
p_0 = probability that $\tau > \tau_c$;
p_m = resuspension rate of cohesive sediment;
p_{m*} = dimensionless resuspension rate of cohesive sediment;
p_{*1}, p_{*2} = dimensionless parameters about resuspension rate;
P = normal stress;

P_m = resuspension mass per unit area per unit time;
r, θ, z = coordinates of cylindrical coordinate system;
R = r-distance from origin;
R_v = resistant force in Fig. 8;
S_* = confronted area of sediments in detachment model;
t = time;
t_0 = characteristic time concerning resuspension phenomena;
t_{01}, t_{02} = characteristic time defined Eqs.(3) and(4);
$\hat{t}_0$ = time scale of fluctuation of bed shear stress;
t_d = duration time required for sediment to be dislodged;
t_p = time to accelerate the particle speed from zero to 90% of v_0;
T_d = time required for sediment to move its diameter length;
u = flow velocity at a level z;
u_c = critical flow velocity;
u_d = local flow velocity at the height of $a_2 d_0$;
u_* = shear velocity;
v = velocity of sediment on detachment;
v_0 = equilibrium velocity of sediment;
V_1 = volume of cohesive material, defined by Eq.(14);
V_2 = volume of transformation of contact sediment;
V_s = volume of the fictitious cube (= ℓ^3);
V_* = volume of contact section in detachment model;
w = water content (%);
w_f = particle's falling velocity given by Stokes law;
y, y_c = $(\tau-\tau)/\sigma_0$ and $(\tau_c-\tau)/\sigma_0$;
α_2 = coefficient in Eq.(13);
δ_0 = variable coefficient of $f(\tau)$;
η, η_1 = viscosities of sediment aggregation;
μ = viscosity of water;
ρ_0 = representative density of sediments at their incipient motion;
ρ_t = apparent density of sediment aggregation, defined by Eq.(8);
σ = real density of sediments;
σ_0 = standard deviation of $f(\tau)$;
τ = bed shear stress (= $\overline{\tau}$ when used in Eqs. 6, 13 and 37 , and in Figs. 3, 4, 9, 10 and 11);
$\overline{\tau}$ = mean value of $f(\tau)$;
τ_c = critical shear sress;
τ_{c1} = shear stress for the limit of sediment particle movement;
τ_{c2} = shear stress for the limit of bed destruction;
τ_{y1} = yield stress of sediment aggregation; and
$\Phi(y)$ = error function.